

Research



Cite this article: Schulz AK, Ning Wu J, Ha SYS, Kim G, Braccini Slade S, Rivera S, Reidenberg JS, Hu DL. 2021 Suction feeding by elephants. *J. R. Soc. Interface* **18**: 20210215. <https://doi.org/10.1098/rsif.2021.0215>

Received: 15 March 2021

Accepted: 11 May 2021

Subject Category:

Life Sciences—Physics interface

Subject Areas:

biomechanics

Keywords:

muscular hydrostat, suction, object manipulation

Author for correspondence:

David L. Hu

e-mail: hu@me.gatech.edu

†Indicates co-first author.

Electronic supplementary material is available online at <https://doi.org/10.6084/m9.figshare.c.5432421>.

Suction feeding by elephants

Andrew K. Schulz^{1,†}, Jia Ning Wu^{1,†}, Sung Yeon Sara Ha¹, Greena Kim¹, Stephanie Braccini Slade³, Sam Rivera⁴, Joy S. Reidenberg⁵ and David L. Hu^{1,2}

¹George W. Woodruff School of Mechanical Engineering, ²School of Biological Sciences, Georgia Institute of Technology, Atlanta, GA 30332, USA

³School of Biology, University of Alabama, Tuscaloosa, AL 35401, USA

⁴Zoo Atlanta, Atlanta, GA 30315, USA

⁵Center for Anatomy and Functional Morphology, Icahn School of Medicine at Mount Sinai, 1 Gustave L. Levy Place, New York, NY 10029-6574, USA

DLH, 0000-0002-0017-7303

Despite having a trunk that weighs over 100 kg, elephants mainly feed on lightweight vegetation. How do elephants manipulate such small items? In this experimental and theoretical investigation, we filmed elephants at Zoo Atlanta showing that they can use suction to grab food, performing a behaviour that was previously thought to be restricted to fishes. We use a mathematical model to show that an elephant's nostril size and lung capacity enables them to grab items using comparable pressures as the human lung. Ultrasonographic imaging of the elephant sucking viscous fluids show that the elephant's nostrils dilate up to 30% in radius, which increases the nasal volume by 64%. Based on the pressures applied, we estimate that the elephants can inhale at speeds of over 150 m s⁻¹, nearly 30 times the speed of a human sneeze. These high air speeds enable the elephant to vacuum up piles of rutabaga cubes as well as fragile tortilla chips. We hope these findings inspire further work in suction-based manipulation in both animals and robots.

1. Introduction

A single African elephant (*Loxodonta africana*) consumes over 200 kg of vegetation daily, spending nearly 18 h d⁻¹ foraging for grass, leaves, fruits and tree bark [1,2] (figure 1a). To grab this variety of items, the elephant relies on its long flexible prehensile trunk [3,4], whose mechanics are still being understood. Elephants are the only extant large terrestrial animal to evolve a long boneless appendage like the trunk [5]. In this study, we investigate how elephants use airflow to pick up items. We characterize the fluid mechanics of elephant suction (duration, speed, pressure) and the numbers and kinds of items that can be grabbed. These variables are measured experimentally by varying the food items and the fluid media. To pump more water, we hypothesize that elephants can increase the storage capacity in their nostril cavities through muscular contraction. Using a mathematical model, we predict the maximum distance that food can be lifted by suction.

Elephants use both air and water as tools to manipulate their environment. In 1871, Darwin reported that elephants blow air to push objects that are just beyond reach [6]. Elephants can modulate the duration of blowing according to the object's distance and can even reflect an air jet off a wall to draw objects closer to themselves [7]. The trunk's flexibility allows it to access water in deep fissures [8] and then spray water over its entire body [9]. Elephants can also use their trunk as a snorkel when traversing deep water [10,11].

Animals that manipulate objects using fluid flow are typically found in water rather than land. The archerfish spits a jet through the water surface to strike airborne insects with great accuracy [12]. It does so by modulating its mouth opening size as it shoots the jet, which increases the force imparted on its target [13]. Squid and octopus use underwater jets to push their bodies at high speed [14–16]. Many fish perform suction feeding, a highly coordinated

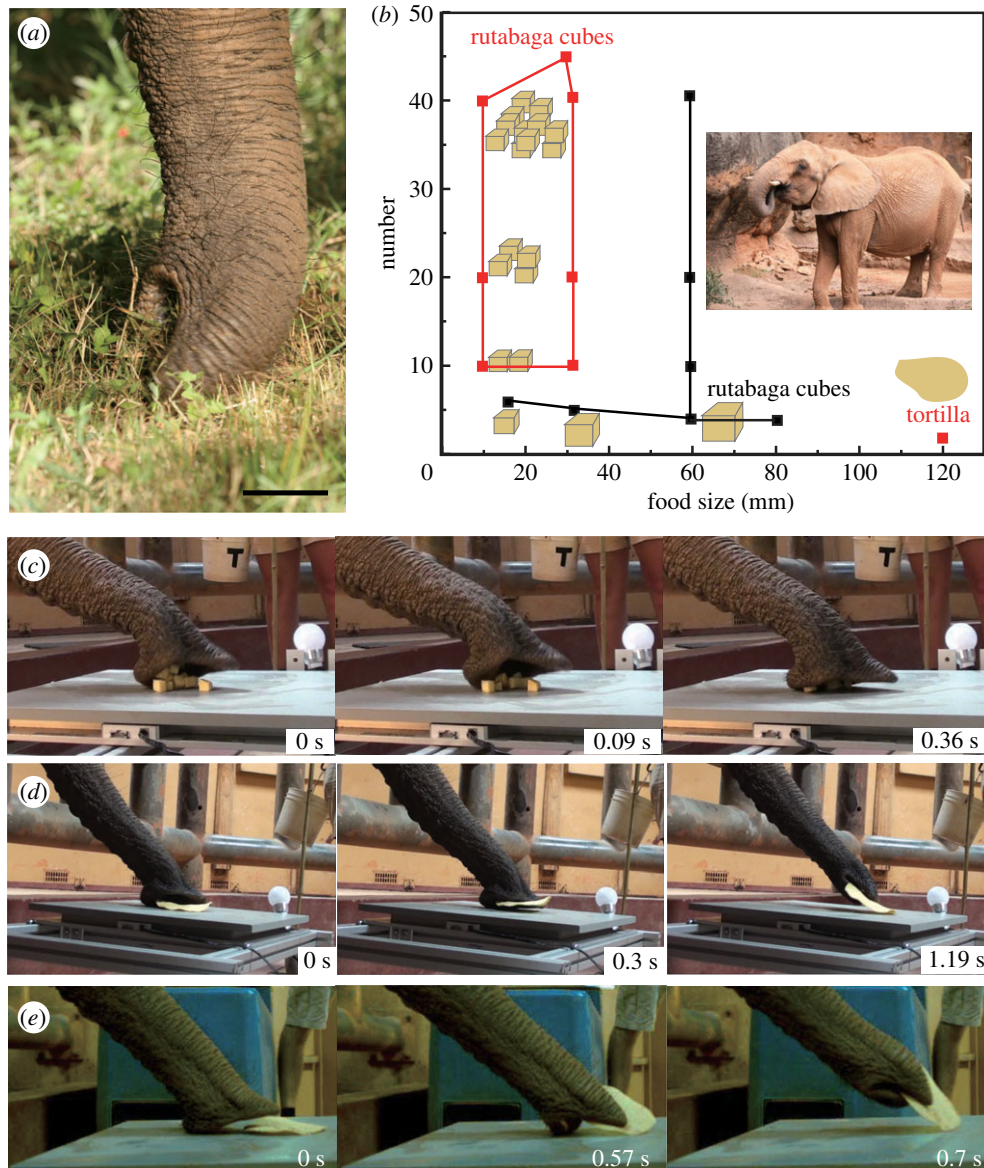


Figure 1. An elephant uses suction to pick up lightweight objects. (a) The trunk of an African elephant, showing its two prehensile ‘fingers’ at the tip of the trunk. Scale bar, 5 cm. (b) A regime diagram for suction across number and size of food items. The red symbols indicate the use of suction and black symbols indicate the absence of suction. The cube-shaped objects are rutabaga cubes and the circular object is a tortilla chip. (c) Elephant picking up ten 16 mm rutabaga cubes using suction. (d) Elephant using suction to levitate a tortilla chip into its grip. (e) Elephant pressing its trunk against a tortilla chip and applying suction to pick it up.

behaviour requiring specialized body parts to quickly generate pressures that draw nearby prey into their mouths [17–19]. Suction feeding is fast and does not require the same precision as physical manipulation of a food item. However, the specialized morphology for suction feeding such as a highly mobile skull makes suction feeding likely restricted to aquatic organisms. Pigs and tapirs use their prehensile snouts for digging and grasping, but it is not known if these activities are enhanced with airflow [20]. In this study, we show that elephants perform their own version of suction feeding without the morphology of fish.

Elephant trunks and octopus arms are appendages consisting of a sheath of skin surrounding muscle fibres. These structures are called muscular hydrostats because their shape is dictated between the opposing forces of the muscle and skin. The dexterity of muscular hydrostats has inspired a number of continuum robots since the 1990s [21–25]. Even the elephant trunk’s transport of water and air has inspired similar functions in robots. One robot can perform autonomous refuelling of ships in various ocean conditions [24]. A search-

and-rescue robot can transport air or water to victims trapped beneath debris [26]. While many of these devices were inspired by the elephant trunk, further knowledge of the elephant’s behaviours may give even more ideas for soft robot design [27].

Beyond elephants, other animals with adhesive capabilities have also inspired robotics. For example, the clingfish uses a modified pelvic disc [28] to stick to slippery rocks underwater using both suction and friction forces. Based on this design, roboticists designed a bioinspired suction cup that can cling to a variety of rough surfaces of varying curvature [29]. Positive and negative pressures have been used in a variety of tasks in industry. When vacuum pressure is coupled with an elastic bag filled with coffee grains, the resulting universal gripper can contort to the shape of a variety of objects [27]. In vehicle manufacturing, vacuum grippers pick up a variety of parts without leaving marks or damage caused by adhesives or other types of manipulation [30]. In other industries, air jets are used to float, levitate, rotate or transport objects [31,32]. Most of these manipulators work on smooth objects like sheets of glass

where a uniform contact is possible. In comparison, the elephant trunk is quite versatile in grabbing a variety of items, as we shall see in our experiments.

In this study, we investigate suction feeding by elephants. We begin in §2 by detailing the experimental methods for observing the elephants grabbing various sized food items. We proceed in §3 with our mathematical model relating the pressure applied by the lungs to the size and weight of the food item that can be retrieved with suction. In §4, we report our results, giving the regime diagram for suction and measurement of pressure generated. In §5, we discuss the implications of our results and predict the range of animals that may also be capable of suction feeding. Concluding remarks are given in §6.

2. Material and methods

2.1. Video of elephant grabbing food items

We performed all experiments at Zoo Atlanta with a 34-year old female African elephant weighing 3360 kg (figure 1*a,b*). All experiments were conducted in the elephant facility at Zoo Atlanta and supervised by the staff at Zoo Atlanta. The experiments occurred over six sessions of 2-h duration at Zoo Atlanta in the summer of 2018.

We performed 42 experiments with different sized rutabaga cubes, cut into side lengths L of 64, 32 and 16 mm. A force plate (Accugait, AMTI, USA) with 1300 N force capacity was used to measure the contact force of the elephant trunk during food intake. The force plate set-up was placed 46 cm from the elephant enclosure allowing the elephant to easily reach the plate (figure 1*c–e*). The cubes were placed evenly on the force platform and in numbers so that each experiment presents the same total mass of food of 200 g. No obstacles were present between the force plate and the elephant enclosure. The set-up is similar to that used in our previous work [4].

Two video cameras (Sony HDRXR200, Japan) were placed in the bird's-eye and side view of the force plate. An indicator light (Massimo Retro LED, USA) with remote control was used to show when the cameras started recording the experiment. A high-speed camera (Phantom M1 10, USA) captured the grabbing of the tortilla chip from the side view.

To perform experiments, the force plate, indicator light and cameras were first installed. The force plate was zeroed and the indicator light was turned on. We placed two types of food, namely, rutabaga and tortilla chips (Charras Corn Tostada, USA) on the centre of the force plate. The zoo staff verbally instructed the elephant to reach for the food. The three cameras started to record the scene and the indicator light was turned off to synchronize the three cameras. Real-time contact force data were captured at the same time.

2.2. Trunk nasal passage measurements

Icahn School of Medicine at Mount Sinai (ISMMS) in New York provided access to a frozen trunk from a 38 year old female African elephant (Specimen ID USNM 590941) that was originally donated from the National Museum of Natural History, Smithsonian Institution. This female elephant was approximately 4000 kg before death, and was euthanized due to medical issues. In this paper, we will refer to this elephant as 'the Smithsonian elephant'. The left nostril is more deformed in the cross sections therefore only the right nostril was used for measurements. The distal tip nostril radius of the Smithsonian elephant was 1.1 cm, which closely matches that of the Atlanta Zoo elephant (1.0 cm). Given the similarity in masses of the two Atlanta and Smithsonian elephants (3360 and 4000 kg), and their trunk nasal

diameters, we will assume that the Smithsonian trunk can be used to approximate dimensions of the Zoo Atlanta elephant.

2.3. Water siphoning measurement and ultrasonographic measurement of trunk wall

A tall aquarium (29.9 × 29.9 × 48 cm) fitted with a ruler was filmed from the front and side using a video camera (Sony Handycam, Japan) at a frame rate of 30 fps. A bag of chia seeds (50 g) was mixed into the water the night before, and the mixture was dropped in the aquarium and then blended evenly with a stirrer before experiments commenced (figure 2*a, b*). Zoo staff led the elephant to the tank by guiding its trunk. For ultrasonographic measurements, the tank was prepared to hold either water (19 l) or water with 500 g of bran.

The trunk wall dimensions were measured at rest and during nasal wall expansion while suctioning liquids of varying density. We used the ultrasound system (MicroMaxx, Sonosite, USA) to measure the thickness of muscle layers surrounding the nasal cavity at two positions, 83.8 and 81.3 cm distal to the margin of the trunk sulcus on the right and left side of the trunk, respectively (figure 3*a,b*). Ultrasound gel (Scan Ultrasound Gel, Parker, USA) was applied to the skin before measurement.

2.4. Phylogenetic analysis of nostril radius

To compare suction ability among mammals, we will report the relationship between nostril radii and body mass for nine mammals as well as a power law best fit that describes the trend. We hypothesize that the trend is due to phylogenetic dependence between the nine species studied. To determine the extent that our trends are influenced by phylogenetic closeness, we performed a phylogenetic independence contrasts (PIC) analysis, a statistical method controlling for the effects of phylogeny [33]. We began by generating a consensus phylogeny using pruned subsets from VertLife including all nine species [34] (electronic supplementary material, figure S1*a*). Using the *pic* function and the package *ape* in R studio, we found that the nostril radius PIC and body mass PIC are not related, and thus phylogenetic dependence of our sample was insignificant ($p = 0.12$; electronic supplementary material, figure S1*b*). However, we note that our small sample size of $n = 9$ may call into question these results, and in the future more animals would need to be measured.

3. Mathematical modelling

We begin by considering the trunk nasal passageways to be that of two conical frustrums, or truncated cones, with total volume V :

$$V(z) = \frac{2\pi z}{3} [(r(z))^2 + r(z)r(0) + r(0)^2], \quad (3.1)$$

where $r(0)$ and $r(z)$ denote the inner radius of trunk at the tip and base, respectively. Of particular interest is the nostril radius at the tip, which we denote by $a = r(0) = 1.1$ cm. Our experiments with the Smithsonian trunk justifies the linear trend for nasal cavity radius.

We next calculate the maximum pressure generated by the elephant's lungs using water intake experiments. The maximum pressure applied is due to simultaneous holding of water of height H in the trunk and suction at speed u_w . This gives rise to a hydrostatic pressure of $\rho_w g H$ and dynamic pressure of $1/2 \rho_w u_w^2$ which can be calculated as

$$P_{\text{lungs}} = -\rho_w g H - 1/2 \rho_w u_w^2 = -20 \text{ kPa} \quad (3.2)$$

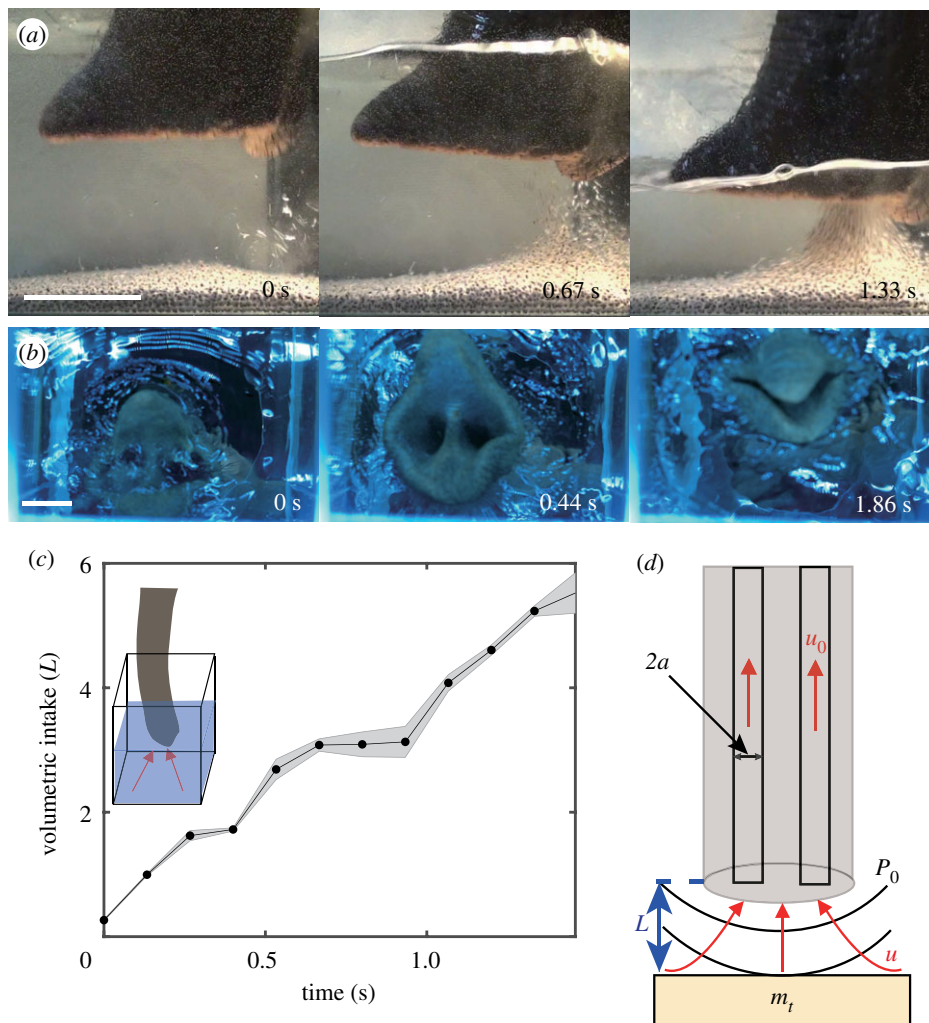


Figure 2. Suction of water. (a) Side view of the elephant siphoning a solution of water mixed with chia seeds acting as flow tracers. Points closest to the nostrils experience the highest speed flow as shown by the trajectory of the chia seeds. Scale bar, 5 cm. (b) Bottom view of elephant siphoning water and closing the trunk to hold the water. Scale bar, 3 cm. (c) Time course of the water flow rate Q . Closed points indicating mean values, and shaded regions show standard deviation. (d) Schematic of an elephant trunk applying suction to a flat object of mass m_t . The red arrows denoted the direction of flow. Nostrils of radius a generate a pressure of P_0 , which generates a flow u_0 in the nasal cavity, and a flow u outside the trunk which rapidly decays with distance L .

where ρ_w is the density of water, g is the acceleration of gravity. The water speed u_w was calculated from the measured flow rate $Q_w = 2\pi a^2 u_w = 3.7 \pm 0.3 \text{ l s}^{-1}$ where a is the nostril radius. The height $H = 190 \text{ cm}$ was extrapolated from the volume V inhaled and the equation (3.1). Based on these measurements, we infer the elephant generates a lung pressure of -20 kPa , which we use below to calculate the maximum distance that a chip can be successfully inhaled.

Consider a tortilla chip at a vertical distance L from the trunk tip as shown in figure 2d. It will rise if the suction force on it, $P(L)A$ exceeds the chip's weight mg :

$$-P(L)A = mg, \quad (3.3)$$

where $P(L)$ is the pressure which decays with distance L , A is the area of one face of the chip and g is the acceleration of gravity. Using conservation of mass, the flow rate at the tip of the trunk, Q_0 , may be written as the product of the area of the two nostrils $2\pi a^2$ and the air velocity u_0 :

$$Q_0 = 2\pi a^2 u_0. \quad (3.4)$$

We apply Bernoulli's equation along three positions along a streamline, the trunk tip, a position L from the tip, and a

position at infinite distance to the trunk tip, arriving at

$$\frac{1}{2}\rho_a u_0^2 + P_0 = \frac{1}{2}\rho_a u^2(L) + P(L) = \frac{1}{2}\rho_a u_\infty^2 + P_\infty = 0, \quad (3.5)$$

where ρ_a is the density of air. Equality with zero is given by the condition at infinity, where air speed u_∞ and pressure P_∞ are both zero. We assume that the air experiences no dissipation as it travels down the trunk, and thus that the pressure at the tip is equal to the lung pressure: $P_0 = P_{\text{lungs}}$. Applying equation (3.5) leads to $u_0 = \sqrt{-2P_{\text{lungs}}/\rho_{\text{air}}} = 150 \text{ m s}^{-1}$, where P_{lungs} is found from our water suction experiments.

Once outside the trunk walls, airspeed decays rapidly with distance due to conservation of mass, which states that flow rate at the tip is equal to flow rate at a distance L : $Q_0 = Q(L)$. Using the flow rate $Q(L)$ at the surface of a sphere of radius L , we write

$$2\pi u_0 a^2 = 4\pi u(L)L^2, \quad (3.6)$$

where $2\pi u_0 a^2$ is the flow rate into the two nostrils. Equation (3.6) may be simplified to: $u(L) = (1/2)u_0 (a^2/L^2)$. Using equation (3.5), the pressure on the surface of the tortilla chip can be expressed as $P(L) = -(1/8)\rho_a u_0^2 (a^4/L^4)$. Using

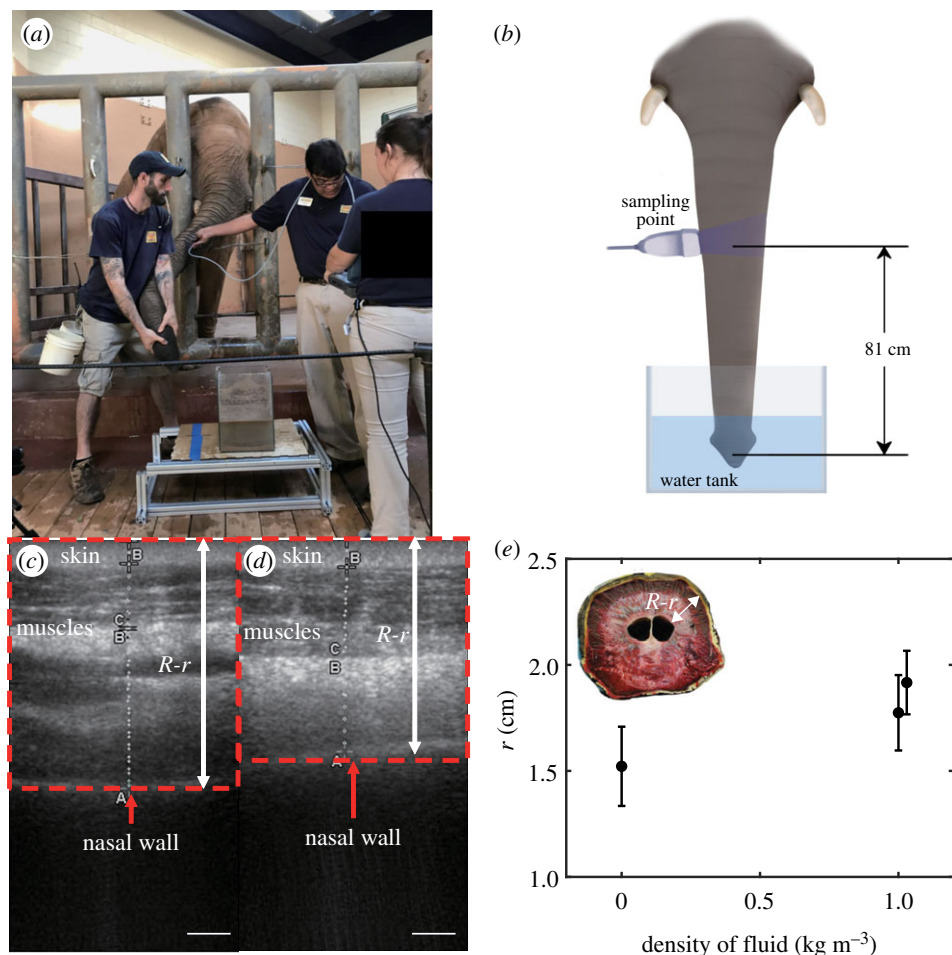


Figure 3. Measurement of nasal wall diameter by ultrasonographic imagery. (a) Set-up for ultrasonographic measurement. (b) Schematic diagram of ultrasonographic measurements collection site. Illustrated by B. Seleb. (c) Ultrasonic image of nasal wall during suction of water. Scale bar, 1 cm. (d) Ultrasonic image of suction of bran water. Scale bar, 1 cm. (e) Relationship between nasal radius r and density of fluid inhaled.

$(1/2)\rho_a u_0^2 + P_0 = 0$ from equation (3.5), we rewrite

$$P(L) = \frac{1}{4} P_0 \frac{a^4}{L^4}. \quad (3.7)$$

The distance L is non-dimensionalized by the nostril radius a . Note that this equation for pressure makes sense: the pressure decreases rapidly with distance L from the nostrils. If the distance is doubled, the pressure goes down by a factor of 32. This expression for pressure may be substituted into equation (3.3), giving us a relationship for the critical height L_c for suction as a function of the lung pressure and nostril radius a :

$$L_c = \left(-\frac{a^4 A P_{\text{lungs}}}{2mg} \right)^{1/4} = Ca, \quad (3.8)$$

where C is a constant and a is the nostril radius.

4. Results

4.1. Suction feeding observations

We fed an elephant rutabaga cubes in varying sizes and quantities in 14 separate experiments. Grabbing behaviour changed with the size and the number of food items offered to the elephant (figure 1b). When given fewer than 10 small cubes (of size smaller than 40 mm), the elephant used the prehensile tip of the trunk, as shown by the black symbols in the regime

diagram without utilizing suction. As the size of the cubes increased in length the elephant continued to use prehensile grabbing. However, if there were more than 10 small items, the elephant employed suction to pick them, as shown by the red symbols. A loud vacuuming sound accompanied the suction as food is quickly drawn onto the tip of the trunk (figure 1c; electronic supplementary material, video S1). In all experiments, the elephant swept its trunk across the force platform to manually contact the food items. When given piles of bran fibre of grain size 1 mm, the elephant did not use suction, presumably to avoid getting the grains lodged in its trunk. Instead, the trunk tip squeezed the bran together to pick them up, as we previously reported [4].

To more clearly see the suction feeding event, we gave the elephant a tortilla chip, representing a flat object in nature such as a broad leaf. The chip is only 500 μm thick, making it challenging to pick up when it sits on a flat surface like the force plate. The force required to break the chip is 11 ± 2 N, which is less than 1% of the trunk weight. After making first contact, the process of picking up the chip took 3.0 ± 0.2 s. As shown in figure 1d,e and electronic supplementary material, video S2, the process involved three phases, including the approach, search and lift. The elephant did not touch the chip directly at first but began by touching the outer edge of the force plate and applying a force of 4 ± 1 N. In the search phase, it approached the chip, pressing with a force of 5 N, which is nearly 50% of the force required to

break the chip. During the lifting phase, the elephant proceeded with two different behaviours. During the first behaviour, the elephant applied suction at a fixed distance from the chip (figure 1*d*). During the second behaviour, the elephant applied suction while pressing the trunk directly onto the chip (figure 1*e*). Even after repeated attempts, the elephant could usually pick it up without breaking it.

4.2. Measurement of pressure and nasal cavity volume

To measure the suction pressure generated, we performed three observations of the elephant sucking water with its trunk. Pre-soaked chia seeds were used to visualize flow patterns generated by the elephant. The flow profile appears parabolic, as shown by the longer distance travelled by the chia seeds at the centre of the nostrils (figure 2*a*). Figure 2*c* shows the time course of the fluid flow into the trunk, as measured by the loss of fluid in the tank. During three trials, the elephant sucked water for 1.5 ± 0.1 s giving an overall flow rate of $Q_w = 3.7 \pm 0.31 \text{ s}^{-1}$, the equivalent of 20 toilets flushing simultaneously. The total liquid volume stored in the trunk was 5.5 ± 0.41 l. The elephant took a half-second break after inhaling 3 l of liquid, during which the flow rate was just $1 \pm 1.21 \text{ s}^{-1}$. Afterward the flow rate increased back up to $4.5 \pm 2.11 \text{ s}^{-1}$ in the last half-second of the suction cycle. This break occurred for all three experiments and we speculate that it is to prevent water penetrating the posterior sphincter in the trunk.

We estimated the nasal cavity volume in the 1.9 m long trunk using data from cross sectional measurements of the trunk. The Smithsonian trunk nasal cavity has 1 cm radii at the distal end and 3 cm at the proximal end. Using a linear fit, we find the nostril inner radius

$$r(z) = 1.1 + 0.02z, \quad (4.1)$$

where all units are in centimetres, and z is the distance from the distal tip. Using equation (3.1), we determine that the total trunk capacity is 5.2 l, which appears close to the inhaled water volume of 5.5 l. We hypothesize that elephants increase their trunk volume further through muscular action. Cross-sectional trunk dissections by Kier [35] show muscles radiating from the nostrils, suggesting a role in volume dilation.

We proceeded by performing ultrasonographic measurements to determine how much the trunk volume can change due to muscle contraction. Ultrasonographic trunk wall measurements were taken during three behaviours: natural breathing in air, inhaling water and inhaling water blended with bran. We repeated each measurement six times. The two ultrasonographic images shown in figure 3*c,d* indicate that the radial muscles contracted when the elephant sucked bran water (electronic supplementary material, video S4).

We assume the original trunk radius R and nostril radius r to be 7.5 and 1.5 cm, respectively, as estimated from the trunk position and the dimensions of the dissected elephant trunk. Thus, the control wall thickness is $R - r = 6$ cm. During the suction of water, the trunk wall thickness $R - r$ was 5.7 cm, where R and r are the outer and inner radius, respectively. For the suction of bran water, the nostrils dilated, and the wall thickness decreased to 5.6 cm. Note that any fluid inhaled or dead-space within the trunk shows up black on the ultrasound, and tissue appears grey. Although we cannot measure all dimensions of nostrils, we will assume uniform dilation and report the new radius of

the nasal passage as $r + \Delta r$, where Δr is the change in thickness of the nasal wall ($R - r$) from its original value of 6 cm.

The nasal radius for sucking air, water and bran water cases are $r = 1.5 \pm 0.2$ cm, 1.8 ± 0.2 cm and 1.9 ± 0.2 cm, respectively, as shown in figure 3*e* and electronic supplementary material, table S3. Compared to their average baseline radius of the Smithsonian elephant trunk, air suction did not lead to any significant changes in diameter. However, sucking water and bran solution led to nostrils increasing in radius by 18% and 28%, respectively, compared to the museum specimen radius. If we assume that all radii along the nasal passages increase the same proportions given above, we may use equation (3.1) to show that trunk capacity increases 40%, and 64% for water and bran solution, respectively. We note that the elephant stopped consuming water after 5.51 voluntarily, indicating that it wants to keep the volume of water no more than 110% of the original trunk nasal passage volume.

4.3. Limits of suction feeding

Now that we have measured the suction pressure and geometry of the trunk, we can apply our mathematical model to predict the effective distance for suction feeding. For our remaining calculations, we use average nasal radius of $a = 2.1$ cm, the average radius along the distal 90 cm of the trunk. We proceed by estimating the maximum pressure applied in the water experiments and in turn, the maximum distance L_c from the chip that the elephant can lift with suction (figure 2*d*).

In our water suction experiments, the average speed of water u_w in the trunk is the flow rate divided by the cross-sectional area of the two nostrils $u_w = Q_w / (2\pi a^2) \sim 2.7 \text{ m s}^{-1}$, in which $a = 2.1$ cm is the nostril radius. The maximum pressure is applied at the end of the suction cycle, in which the water is at its highest speed and height in the trunk. By calculating the Reynolds number of the flow inside the elephant trunk nostril, we can estimate if the fluid is experiencing turbulence. The Reynolds number of transporting water through a pipe is $Re_w = 2\rho_w u_w r / \mu_w = 8.1 \times 10^4$, and the Reynolds number for air is $Re_a = 4.2 \times 10^6$. These Reynolds numbers exceed 4000, which indicates that using Bernoulli's Law is a good approximation. By applying Bernoulli's Law as in the math methods section, we find that the pressure applied is -20 kPa. If a similar pressure is applied during chip suction, we calculate using equation (3.5) that the air velocity would be 150 m s^{-1} .

Equation (3.8) shows that the distance L_c that an elephant can suck an object scales linearly with the nostril size ($L_c \sim a$). An object with a lighter mass or greater surface area can be even further from the nose and still be sucked in successfully. Using our measurements of tortilla chip surface $A = 113 \text{ cm}^2$, tortilla mass $m = 10$ g, the acceleration of gravity $g = 9.81 \text{ m s}^{-2}$, and our measured lung pressure $P_{\text{lungs}} = -20$ kPa, we predict a critical height of 4.6 cm, whose range encompasses the experimental value of 4 ± 0.5 cm ($n = 5$).

5. Discussion

A critical factor for elephants to suction feed is their lung pressure. Elephants can generate such high lung pressures because of their specialized respiratory system [36]. A distensible network of collagen fibres fills the pleural space, loosely connecting the lungs to the chest wall but appears not to constrain lung–chest wall movements [36–38]. This anatomical

structure contributes to such a high air velocity that makes the suction-aided manipulation possible. It has been shown that the endothoracic fascia in elephants is eight times as thick as that of humans, rabbits, rats and mice which could allow for the added pressure in their lungs [39]. This anatomical differences are possible reasons elephants could generate such high air velocities of 150 m s^{-1} , which is 30 times the spray speed of a human cough or sneeze (4.5 m s^{-1}) [37,40], and comparable to the speed of a high-speed rail train (150 m s^{-1} , AGV, France) [38].

Can other animals also lift food items by suction? Using previous measurements of nine mammals [41–48], the relationship between body mass M and nostril radius a is shown by figure 4a, with the power law best fit

$$a = 1.85M^{0.29} \quad (R^2 = 0.88), \quad (5.1)$$

where a is in mm and M is in kg. The exponent is positive indicating that nostril radius increases with body size. Since closely related species tends might have similar nostril radii, we performed statistical analysis to determine if the trend is due to phylogenetic closeness (see Material and methods). We find a p -value of 0.12, indicating that data dependence caused by phylogeny is likely insignificant, but we also note that our sample size of nine may be too small to draw conclusions.

Elephants have the widest nostrils of any mammal we examined, with a nostril radius ranging from 10 mm at the tip to 30 mm at a distance of 90 cm from the distal tip. An elephant has a nasal radius that 100 times that of a mouse (0.21 mm nasal radius) [49], and two times that of a human at the distal tip (nasal radius of 5 mm) [50]. Using the approximation [51] that lung pressure applied by animals is constant at -10 kPa , we apply equation (3.8) to estimate the maximum distance for animals to pick up the same tortilla chip in our experiments. Figure 4b and the electronic supplementary material, table S1 shows the critical height across body mass. After the elephant, the second most massive animal is the cow, which has a critical height of 1 cm, indicating they must nearly press their nose to the chip to lift it. Pigs and tapirs would need to be within 0.65 cm of tortilla chips to lift objects. This indicates pigs and tapirs likely only use suction for very small objects if at all.

Could a human pick up items by suction? Yes, but only items as light as a small piece of paper. According to allometric estimates, lung vital capacity increases at a rate of 6.3 ml kg^{-1} of body weight [52]. Therefore an elephant's lungs are many times that of human lungs in vital capacity. While humans can generate the same lung pressure as elephants, applying equation (3.8) we find that a human's lung volume and nostril diameter are large enough to only lift a small piece of paper. A human's nose would have to get within 0.4 mm of the tortilla chip to lift the chip with suction. Moreover, any fluid leaks between the chip and nose would make lifting infeasible.

When elephants pick up an item, they can simultaneously touch and smell it, a feat that we cannot perform with the human hand. An elephant has a strong sense of smell, and can detect the smell of TNT with higher accuracy than most bomb detection dogs [53]. The elephant ability to reach for objects may be impaired if the elephant holds a stick with its trunk, which impairs its ability to use olfaction [54].

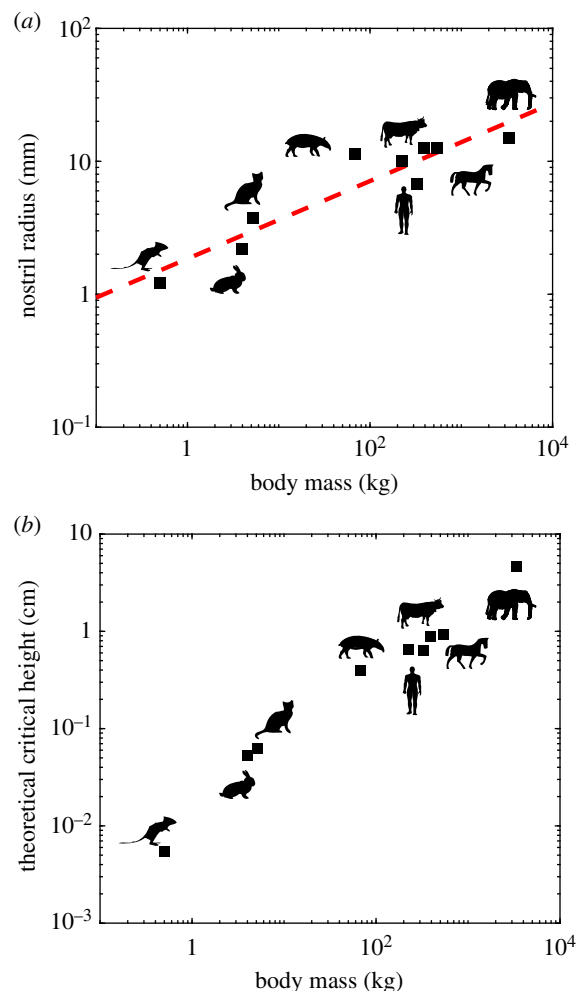


Figure 4. Predicted suction feeding across terrestrial animals. (a) Relationship between nostril radius and body mass, with power law fit shown by the red line. (b) Relationship between body mass and the theoretical distance L_c to pick up a tortilla chip. Animal portraits from Adobe Creative Studio.

Future workers may find that elephants use olfaction to generate a three-dimensional picture of the world.

6. Conclusion

In this study, we investigated suction feeding by elephants. We showed that elephants employ this behaviour for large numbers of small items as well as for single flat items like tortilla chips. Using liquid suction experiments, we measured the pressure that elephants generated and showed that elephants can expand the volume of their trunk by up to 64% to carry more water. Previously suction feeders were thought to be mainly underwater, and this work shows that this behaviour has a broader generality. In robotics, suction has long been used to grab objects. The behaviours shown here may give further inspiration on the usage and design of such devices.

Ethics. In working with animals from Zoo Atlanta. We received research permits from both Zoo Atlanta and Georgia Institute of Technology. The experiments performed were approved under Zoo Atlanta permit Matter transport by elephant trunks. The experiments performed were approved under Georgia Tech IACUC A16032.

Data accessibility. Measurement data provided in the electronic supplementary material file and a github repository.

Authors' contributions. A.K.S. performed experiments, data analysis and wrote the manuscript for submission. J.N.W. performed experiments and wrote manuscript for submission. S.Y.S.H. performed experiments.

G.K. performed experiments. S.B.S. helped perform experiments and provided input on elephant experiments. S.R. helped with ultrasonographic imagery of elephant suction experiments. J.S.R. assisted with dissection of elephant trunk and measurements of nasal cavity. D.L.H. is corresponding author responsible for the majority of the edits of the publication as well as hypothesis testing.

Competing interests. We declare we have no competing interests.

Funding. This work was supported by the US Army Research Laboratory and the US Army Research Office Mechanical Sciences Division, Complex Dynamics and Systems Program, under contract number W911NF-12-R-0011.

Acknowledgements. We thank the Zoo Atlanta elephant keepers for helping us conduct the elephant's grabbing experiments. We thank Kelsie Pos for helping us with the phylogenetic closeness analysis.

References

- Boas T, Paulli S. 1925 *The elephant's head, part 2*. Copenhagen, Denmark: The Carlsberg Fund.
- Ullrey DE, Crissey SD, Hintz HF. 1997 *Elephants: nutrition and dietary husbandry*. Nutrition Advisory Group.
- Shoshani J. 1998 Understanding proboscidean evolution: a formidable task. *Trends Ecol. Evol.* **13**, 480–487. (doi:10.1016/S0169-5347(98)01491-8)
- Wu J, Zhao Y, Zhang Y, Shumate D, Slade SB, Franklin SV, Hu DL. 2018 Elephant trunks form joints to squeeze together small objects. *J. R. Soc. Interface* **9**.
- Pretorius Y, de Boer WF, Kortekaas K, van Wijngaarden M, Grant RC, Kohi EM, Mwakiwa E, Slotow R, Prins HHT. 2016 Why elephant have trunks and giraffe long tongues: how plants shape large herbivore mouth morphology. *Acta Zoologica* **97**, 246–254. (doi:10.1111/azo.12121)
- Darwin C. 1871 *The descent of man*. London, UK: John Murray.
- Mizuno K, Irie N, Hiraiwa-Hasegawa M, Kutsukake N. 2016 Asian elephants acquire inaccessible food by blowing. *Anim. Cogn.* **19**, 215–222. (doi:10.1007/s10071-015-0929-2)
- Wyatt JR, Eltringham SK. 1974 The daily activity of the elephant in the Rwenzori National Park, Uganda. *African J. Ecol.* **12**, 273–289. (doi:10.1111/j.1365-2028.1974.tb01037.x)
- Garstang M, Du Plessis W, Du Plessis C. 2015 *Elephant sense and sensibility: behavior and cognition*. London, UK: Academic Press.
- O'bryhim S. 1991 Hannibal's elephants and the crossing of the Rhône. *Class. Quart.* **41**, 121–125. (doi:10.1017/S000983880003591)
- West JB. 2001 Snorkel breathing in the elephant explains the unique anatomy of its pleura. *Respir. Physiol.* **126**, 1–8. (doi:10.1016/S0034-5687(01)00203-1)
- Dewenter J, Gerullis P, Hecker A, Schuster S. 2017 Archerfish use their shooting technique to produce adaptive underwater jets. *J. Exp. Biol.* 1019–1025.
- Gerullis P, Schuster S. 2014 Archerfish actively control the hydrodynamics of their jets. *Curr. Biol.* **24**, 2156–2160. (doi:10.1016/j.cub.2014.07.059)
- O'Dor R, Stewart J, Gilly W, Payne J, Borges TC, Thys T. 2013 Squid rocket science: how squid launch into air. *Deep Sea Res. Part II* **95**, 113–118. (doi:10.1016/j.dsr2.2012.07.002)
- Sumbre G, Fiorito G, Flash T, Hochner B. 2005 Neurobiology: motor control of flexible octopus arms. *Nature* **433**, 595–596. (doi:10.1038/433595a)
- Wells MJ. 2013 *Octopus: physiology and behaviour of an advanced invertebrate*. Berlin, Germany: Springer Science & Business Media.
- Beckert M, Flammang BE, Nadler JH. 2015 Remora fish suction pad attachment is enhanced by spinule friction. *J. Exp. Biol.* **218**, 3551–3558. (doi:10.1242/jeb.123893)
- Camp AL, Roberts TJ, Brainerd EL. 2015 Swimming muscles power suction feeding in largemouth bass. *Proc. Natl Acad. Sci. USA* **112**, 8690–8695. (doi:10.1073/pnas.1508055112)
- Lauder GV. 1980 The suction feeding mechanism in sunfishes (*Lepomis*): an experimental analysis. *J. Exp. Biol.* **88**, 49–72. (doi:10.1242/jeb.88.1.49)
- Milewski AV, Dierenfeld ES. 2013 Structural and functional comparison of the proboscis between tapirs and other extant and extinct vertebrates. *Integrative Zool.* **8**, 84–94. (doi:10.1111/j.1749-4877.2012.00315.x)
- Cieslak R, Morecki A. 1999 Elephant trunk type elastic manipulator—a tool for bulk and liquid materials transportation. *Robotica* **17**, 11–16. (doi:10.1017/S0263574799001009)
- Grzesiak A, Becker R, Verl A. 2011 The bionic handling assistant: a success story of additive manufacturing. *Assembly Automation* **31**, 329–333. (doi:10.1108/01445151111172907)
- Hannan MW, Walker ID. 2003 Kinematics and the implementation of an elephant's trunk manipulator and other continuum style robots. *J. Robot. Systems* **20**, 45–63. (doi:10.1002/rob.10070)
- Scott GP, Henshaw CG, Walker ID, Willimon B. 2015 Autonomous robotic refueling of an unmanned surface vehicle in varying sea states. In *2015 IEEE/RSJ Int. Conf. on Intelligent Robots and Systems (IROS), Hamburg, Germany*, pp. 1664–1671. New York, NY: IEEE.
- Wilson JF, Li D, Chen Z, George RT. 1993 Flexible robot manipulators and grippers: relatives of elephant trunks and squid tentacles. In *Robots and biological systems: towards a new bionics?* (eds P Dario, G Sandini, P Aebischer), NATO ASI Series, pp. 475–494. Berlin, Germany: Springer.
- Tsukagoshi H, Kitagawa A, Segawa M. 2001 Active Hose: an artificial elephant's nose with maneuverability for rescue operation. In *Proc. 2001 ICRA. IEEE Int. Conf. on Robotics and Automation (cat. no. 01CH37164)*, vol. 3, pp. 2454–2459.
- Brown E, Rodenberg N, Amend J, Mozeika A, Steltz E, Zakin MR, Lipson H, Jaeger HM. 2010 Universal robotic gripper based on the jamming of granular material. *Proc. Natl Acad. Sci. USA* **107**, 18 809–18 814. (doi:10.1073/pnas.1003250107)
- Maie T, Schoenfuss HL, Blob RW. 2012 Performance and scaling of a novel locomotor structure: adhesive capacity of climbing gobiid fishes. *J. Exp. Biol.* **215**, 3925–3936. (doi:10.1242/jeb.072967)
- Sandoval JA, Jadhav S, Quan H, Deheyn DD, Tolley MT. 2019 Reversible adhesion to rough surfaces both in and out of water, inspired by the clingfish suction disc. *Bioinspir. Biomimet.* **14**, 066016. (doi:10.1088/1748-3190/ab47d1)
- Callies R, Fronz S. 2008 Recursive modeling and control of multi-link manipulators with vacuum grippers. *Math. Comput. Simul.* **79**, 906–916. (doi:10.1016/j.matcom.2008.02.003)
- Li X, Guo Z, Kagawa T. 2015 Development and experimental evaluation of air flotation element with additional air-intake capacity. *Lubr. Sci.* **27**, 397–411. (doi:10.1002/lis.1294)
- Paivanas JA, Hassan JK. 1976 Air film system for handling semiconductor wafers. *IBM J. Res. Dev.* **15**.
- Felsenstein J. 1985 Phylogenies and the comparative method. *Am. Nat.* **125**, 1–15. (doi:10.1086/284325)
- Upham NS, Esselstyn JA, Jetz W. 2019 Inferring the mammal tree: species-level sets of phylogenies for questions in ecology, evolution, and conservation. *PLoS Biol.* **17**, e3000494. (doi:10.1371/journal.pbio.3000494)
- Kier WM, Smith KK. 1985 Tongues, tentacles and trunks: the biomechanics of movement in muscular-hydrostats. *Zool. J. Linnean Soc.* **83**, 307–324. (doi:10.1111/j.1096-3642.1985.tb01178.x)
- Brown RE, Butler J, Godleski J, Loring S. 1997 The elephant's respiratory system: adaptations to gravitational stress. *Respir. Physiol.* **109**, 177–194. (doi:10.1016/S0034-5687(97)00038-8)
- Bourouiba L, Dehandschoewercker E, Bush JW. 2014 Violent expiratory events: on coughing and sneezing. *J. Fluid Mech.* **745**, 537–563. (doi:10.1017/jfm.2014.88)
- Campos J, De Rus G. 2009 Some stylized facts about high-speed rail: a review of HSR experiences around the world. *Transport Policy* **16**, 19–28. (doi:10.1016/j.tranpol.2009.02.008)
- West JB, Fu Z, Gaeth AP, Short RV. 2003 Fetal lung development in the elephant reflects the adaptations required for snorkeling in adult life. *Respiratory Physiol. Neurobiol.* **138**, 325–333. (doi:10.1016/S1569-9048(03)00199-X)
- Tang JW *et al.* 2013 Airflow dynamics of human jets: sneezing and breathing—potential sources of infectious aerosols. *PLoS ONE* **8**.
- Fox J. 2006 *The mouse in biomedical research: normative biology, husbandry, and models*. Burlington, MA: Academic Press.

42. Franzmann AW, Schwartz CC, Johnson DC. 1984 Baseline body temperatures, heart rates, and respiratory rates of moose in Alaska. *J. Wildl. Dis.* **20**, 333–337. (doi:10.7589/0090-3558-20.4.333)
43. Gajic O *et al.* 2004 Ventilator-associated lung injury in patients without acute lung injury at the onset of mechanical ventilation. *Crit. Care Med.* **32**, 1817–1824. (doi:10.1097/01.CCM.0000133019.52531.30)
44. Gallivan GJ, McDonnell WN, Forrest JB. 1989 Comparative pulmonary mechanics in the horse and the cow. *Res. Vet. Sci.* **46**, 322–330. (doi:10.1016/S0034-5288(18)31174-3)
45. Medici P, Traeholt C, Tobler M, Silva A, Lizcano D, Colbert M, Pukazhenthil B, Thoisy B, Seitz S. 2013 The Newsletter of the IUCN/SSC tapir specialist group. *Tapir Conservation*. See <https://ufdc.ufl.edu/UF00095885/00031>.
46. Praag V. 2003 Anesthesia of the rabbit. Part I: pre-anesthetic preparations. In *Surgery in Rabbits* 4. See http://www.medirabbit.com/EN/Surgery/Anesthesia_rabbits_pre.
47. Simoes EA, Roark R, Berman S, Esler LL, Murphy J. 1991 Respiratory rate: measurement of variability over time and accuracy at different counting periods. *Arch. Dis. Child.* **66**, 1199–1203. (doi:10.1136/adc.66.10.1199)
48. Stahl WR. 1967 Scaling of respiratory variables in mammals. *J. Appl. Physiol.* **22**, 453–460. (doi:10.1152/jappl.1967.22.3.453)
49. Jacob A, Chole RA. 2006 Survey anatomy of the paranasal sinuses in the normal mouse. *Laryngoscope* **116**, 558–563. (doi:10.1097/01.MLG.0000202085.23454.2F)
50. Schriever VA, Hummel T, Lundström JN, Freiherr J. 2013 Size of nostril opening as a measure of intranasal volume. *Physiol. Behav.* **110–111**, 3–5. (doi:10.1016/j.physbeh.2012.12.007)
51. Kim W, Bush JW. 2012 Natural drinking strategies. *J. Fluid Mech.* **705**, 7–25. (doi:10.1017/jfm.2012.122)
52. Villar J, Kacmarek RM. It does not matter whether you are an elephant or a shrew: all mammals' tidal volumes are similarly scaled! *Minerva Anestesiologica* **80**, pp. 5.
53. Miller AK, Hensman MC, Hensman S, Schultz K, Reid P, Shore M, Brown J, Furton KG, Lee S. 2015 African elephants (*Loxodonta africana*) can detect TNT using olfaction: implications for biosensor application. *Appl. Anim. Behav. Sci.* **171**, 177–183. (doi:10.1016/j.applanim.2015.08.003)
54. Foerder P, Galloway M, Barthel T, Iii DEM, Reiss D. 2011 Insightful problem solving in an Asian elephant. *PLoS ONE* **6**, e23251. (doi:10.1371/journal.pone.0023251)